JURNAL KIMIA VALENSI
p-ISSN: 2460-6065; e-ISSN: 2548-3013
Journal homepage: https://journal.uinjkt.ac.id/index.php/valensi
Research Article

Inhibition of Human Acetylcholinesterase (4EY7) using Bioactive Compound from *Moringa oleifera*: Molecular Docking and Dynamic Studies

Wiji Utami[1*], Apriyanto[2], Laila Antari[3], Herlina Rasyid[4], Ika Nur Fitriani[5,6]

[1,3]*Chemistry Department, Faculty of Science and Technology, UIN Sulthan Thaha Saifuddin, Jambi, 36361, Indonesia*
[2]*Faculty of Medicine, UIN Sulthan Thaha Saifuddin Jambi, Jambi, 36361, Indonesia*
[4]*Chemistry Department, Faculty of Mathematics and Natural Sciences, Hasanudin University, Makassar, 90245, Indonesia*
[5]*Chemistry Department, Faculty of Science and Technology, UIN Walisongo, Semarang, 50185, Indonesia*
[6]*School of Chemistry, The University of Sydney, Sydney, Australia*

[*]*Email: wijiutami@uinjambi.ac.id*

Article Info
Received: June 29, 2024
Revised: June 29, 2024
Accepted: Dec 16, 2024
Online: Dec 25, 2024

Citation:
Utami, W., Apriyanto., Antari, L., Rasyid, H., Fitriani, I. K. (2024). Inhibition of Human Acetylcholinesterase (4EY7) using Bioactive Compound from *Moringa oleifera*: Molecular Docking and Dynamic Studies. *Jurnal Kimia Valensi*, 10(2), 290-303.

Doi: 10.15408/jkv.v10i2.39840

Abstract

Alzheimer's disease is a neurodegenerative disorder caused by acetylcholine hydrolysis that impairs cognitive brain function. This research aims to determine the interaction and dynamic of ligands from *Moringa oleifera* on AChE through Lipinski's Rule, ADMET properties, molecular docking calculations, and molecular dynamic simulations. Lipinski's Rule calculation provided ligand limits that adhere to druglikeness properties. ADMET results also showed that several ligands satisfy ADMET properties. Pterygospermine has lower binding energy than the ligand control (-10.28 kcal mol^{-1}) with amino acid residues of TYR133 and GLU202. It indicates a favorable interaction between the AChE receptor and ligand in the inhibition process. Based on molecular docking calculations, pterygospermine inhibits the AChE receptor at the Long, narrow aromatic gorge active site. According to molecular dynamic simulations, the MMPBSA energy for pterygospermine is 37.377 kJ mol^{-1}. The samples showed a total average RMSD of 2 Å, suggesting no significant conformational changes throughout the simulation. The sample's average RMSF value is around 2 Å, suggesting favorable interactions with the receptor during simulation. However, this data is different from the ligand control interaction mode. Molecular dynamic investigations of the pterygospermine ligand in the complex revealed the stability and unfolded effect on the protein. The results of this study propose a candidate anti-Alzheimer's ligand from *Moringa oleifera* against the AChE receptor. In practice, these results can contribute to research studies exploring natural ingredients from plants with medicinal potential in drug discovery. These results can be validated using further research in vitro and in vivo.

Keywords: Acetylcholinesterase, molecular docking, molecular dynamic, *Moringa oleifera*, pterygospermine

1. INTRODUCTION

Alzheimer's is a neurodegenerative disorder that progressively hinders brain function in humans [1]. Alzheimer's disease is triggered by the presence of *Acetylcholinesterase* (AChE) that hydrolyzes acetylcholine into choline and acetate, disturbing the brain's neuron system [2]. In the absence of treatment for this disease, symptoms are susceptible to dementia. A patient with Alzheimer's exhibits traits including memory impairment, issues thinking and reasoning, diminished language, and behavioral fluctuations [3]. The alternative treatment for Alzheimer's in clinical practice commonly involves synthetic drugs like rivastigmine, donepezil, neostigmine, and tacrine [4,5].

These drugs have been demonstrated to be effective AChE inhibitors. However, they may cause side effects such as diarrhea, vomiting, syncope, bradycardia, and nausea [6]. These medications have modest drug performance and only reduce symptoms[6]. However, the therapeutic for alzheimer's disease in clinical practice was used as a model for creating new medications. Therefore, developing novel medicines derived from secondary metabolites of medicinal plants is critical because bioactive molecules have a broad spectrum of bioactivity [2]. The FDA has accepted the discovery of galanthamine, an AChE inhibitor from *Galanthus woronowi* [7]. However, the potential of other plants needs to be studied to obtain other AChE inhibitor candidates. Other plants studied as potential AChE inhibitors are *Rosa damascene* Herrm, *Picrasma quassoides* (D.Don) Benn, *Actinidia arguta* (Siebold & Zucc.) Planch. ex Miq, *Cassia obtusifolia* L., *Markhamia tomentosa* (Benth.) K. Schum. ex Engl., *Rheum ribes* L., *Piper nigrum* L., and *Alpinia galanga* (L.)[8]. All study findings are constantly refined to achieve the most significant outcomes. The study of anti-alzheimer from medicinal plants is a potential future drug candidate [9]. Moringa leaves have a higher nutritional content than other medicinal plants, which are called miracle trees. *Moringa oleifera* is among the medicinal herbs that suppress AChE in Alzheimer's.

Moringa oleifera is traditionally applied as a medication in society. The liquid extracted from the bark has been utilized to cure meningitis. In addition, a decoction of *Moringa oleifera* root has been administered to treat female hysteria and epilepsy [10]. *Moringa oleifera* is a medicinal plant with rich benefits such as neuroprotective [11], antilipase, anti-AChE [12], anti-inflammatory, anti-tumor, anti-neuroinflammatory[13], anticancer, liver protection, regulate enzyme activity, modulate blood glucose, induce cell cycle arrest, and apoptosis [14]. Because of the fascinating benefits of *Moringa oleifera*, this plant has been developed as a new drug for alzheimer disease. *Moringa oleifera* includes secondary metabolites, notably phenolics, flavonoids, tannins, vitamin C, and alkaloids. Antioxidants in this medical plant also avert free radicals that attack nerve cells. Quercetin on extract was proven to inhibit the AChE enzyme [15]. Previous studies reported that the extract of hexane solvent root revealed a high anti-AChE of 1.86 ± 0.06 mg ml^{-1} [12].

Furthermore, the leaf extract of *Moringa oliefera* using methanol and ethyl acetate has also proven an inhibition ability to AChE and butyrylcholinesterase (BChE) [16]. Djiogue et al. (2022) also appended information that could prevent hippocampus nerve loss in test animals [11]. They also claimed that this extract has neuroprotective [13], antioxidant, and memory-protective functions [11,17]. Alkaloids have been used to treat a variety of ailments for thousands of years. Huperzine A has been shown to increase memory in test animals and can traverse the BBB. Furthermore, physostigmine may enhance the memory of dementia patients [18] . This chemical has a longer AChE inhibitory action than tacrine or donepezil. Alkaloids can inhibit Alzheimer's disease by forming neurofibrillary tangles, inhibiting amyloid beta (Aβ), inhibiting pro-inflammatory factors, stabilizing the nicotinic acetylcholine receptor allosteric site (nAChR), and inhibiting AChE [3]. An alkaloid content on *Moringa oleifera* has mitigated oxidative pressure and inflammation [19].

Compounds produced from *Moringa oleifera* have been studied in vitro and in vivo for their ability to diminish Alzheimer's pathology and other Alzheimer's-like cognitive impairments. Moringa extract can lower tau hyperphosphorylation and Aβ levels in rat models. This plant extract's methanol also exhibited neuroprotective properties in Wistar rats that have been sub-chronically exposed to chlorpyrifos. Furthermore, a 70% ethanol extract showed the ability to decrease scopolamine-induced cognitive impairment in mice [17,20,21]. However, no comprehensive investigation employing an in silico technique has yet been conducted. Currently, the utilization of an in silico approach to drug discovery is a promising field because it is efficient, fast, and inexpensive[22]. As a result, the potential of bioactive chemicals isolated from *Moringa oliefera* as AChE inhibitors was investigated using the Lipinski Rule of Five, ADMET properties, molecular docking calculation, and molecular dynamics simulation. In theory, natural and pharmaceutical researchers might utilize this data as a predictor while developing Alzheimer's therapies to reduce failure. In practice, the findings of this study could be applied to carry out additional research on *Moringa oleifera* medicinal plants.

2. RESEARCH METHODS

Lipinski's Rules of Five and ADMET Studies

Lipinski's Rule of Five aimed to evaluate bioactive compounds derived from *Moringa oliefera* as drug candidates that fulfilled the rule of druglikeness. Bioactive compounds that adhere to Lipinski's rules have physic-chemistry properties for oral administration in humans. The rules are molecular weight ≤500 Da, the partition coefficient of octanol/water (MlogP) ≤5, Hydrogen Bond Acceptor (HBA) ≤10, and Hydrogen Bond Donor (HBD) ≤5 [8]. Bioactive compounds that adhere to Lipinski's Rule of Five will be calculated using a molecular docking study. Furthermore, the ADMET prediction is used to obtain the pharmacokinetics of the drug candidate from *Moringa oliefera*. The information from ADMET prediction is % Human Intestinal Absorption (HIA), Carcinoma Colon-2 (Caco-2) cell, % Plasma

Protein Binding (PPB), Blood blood-brain barrier (BBB), mutagen, and carcinogen [23]. To obtain data for this study, several computational applications were used in the form of website-based applications, namely http://www.scfbio-iitd.res.in/software/drugdesign/lipinski.jsp#anchortag (accessed on 12 January 2024) to explore the druglikeness of drug candidate ligands [24,25]. ADMET predictions were screened by inputting compound to web-based software https://preadmet.webservice.bmdrc.org/ accessed on 7 January 2024 [26,27].

Molecular Docking Calculation

Molecular docking calculation was conducted to investigate the binding energy of ligand-receptor complexes and other properties. The targeted protein from the PDB database (https://www.rcsb.org/) is ID 4EY7. From now on, twenty-five bioactive compounds derived from *Moringa oliefera* were retrieved from PubChem (https://pubchem.ncbi.nlm.nih.gov/). The structure of this study was prepared using Chimera 1.14 [28]. This material preparation was performed to add hydrogen and charge to molecular compounds utilizing the standard AMBER FF14SB and Gasteiger residues. If all the molecules were prepared, the method validation is a crucial step through redocking. Redocking was performed utilizing rivastigmine as a reference ligand. This drug was located on the receptor's active site to obtain binding energy and amino acid residue data. Rivastigmine was chosen as the reference ligand because this drug has a shorter half-life than other drugs, such as donepezil and galantamine [29].

Moreover, this drug was accepted by the Food Drug Administration of the United States of America as anti-Alzheimer. Molecular docking calculation was performed using AutoDockTools 1.5.6 [16]. Molecular docking calculation was conducted in a grid box of $68 \times 72 \times 68$ with a spacing of 0.375 Å using 10 Lamarckian Genetic Algorithm runs [30]. The complexes of molecular docking results were visualized using Biovia Discovery Studio to obtain amino acid residue on the active site collect residue amino acids[31]. The complexes of molecular docking results were visualized using Biovia Discovery Studio to obtain amino acid residue on the active site.

Molecular Dynamic Simulation

The molecular dynamics simulation protocol was performed for the ligand-AChE complex, which resulted from molecular docking calculations. The ligand is pterygospermine, with lower binding energies than the control ligand. Next, the molecular dynamics simulation results were compared with the molecular dynamics calculations of the control ligand, namely the rivastigmine-AChE complex. A simulation was performed using the YASARA Structure Program developed by Bioscience GmBH, Vienna, Austria[32]. The first step was to input each sample into the program through Option. Then, Macro & Movie menus were selected, and the Set Target was selected as the last step. Molecular dynamics simulation was carried out with the YASARA Structure program developed by Biosciences GmbH. The molecular dynamics simulation used the protein-ligand complex resulting from molecular docking as an input file. Protein complexes (AChE) with ligands (Rivastugmine and Pterygospermine) in pdb file format are subjected into the Yasara Structure Program in the Options menu and then selected the Macro & Movie menu, which is then simulated using md_run.mcr with the target in the form of a protein complex and ligand pdb file of each compound. The simulation begins with minimizing the potential energy; temperature about 310 K, and pH of 7.4. This condition is regulated to adjust to the physiological conditions of the human body so that the simulations carried out have similarities with these physiological conditions [33].

Furthermore, input macro was performed to conduct molecular dynamic simulation using a prepared sample. In the next step, a running time was set on macro md_run of 50,000 ps (50 ns). In the Yasara Structure program, the forcefield used is Amber14 with intermolecular forces calculated every 2 fs and intramolecular forces calculated every 1 fs [33]. Trajectory data is carried out every 25 ps and data analysis is carried out in the form of potential energy analysis, number of hydrogen bonds in the solute, number of hydrogen bonds between solute and solvent, RMSD, and radius of gyration obtained by running macro md_analyze.mcr. Furthermore, the RMSF analysis was carried out with a macro of md_analyzeres.mcr, while for the study of Molecular Mechanics Poisson-Boltzmann Surface Area (MMPBSA), a macro of md_analyzebindenergy.mcr was used. Data production is carried out after 5 ns from the simulation time to the simulation time of 50 ns, the longer the simulation is carried out, the better the data analysis obtained. One of the parameters used to determine the simulation time is the RMSD analysis data. If the protein and ligand complexes do not experience significant fluctuations, then the simulation time can be stopped at a time range of 50 ns.

The analysis of potential energy, number of hydrogen bonds in the solute, number of hydrogen bonds between solute and solvent, RMSD, and radius of gyration were obtained by running a macro md_analyze. Data was analyzed using the RMSD, RMSF, and Radius of Gyration metrics. These three variables may be used to predict the stability of protein

and ligand complexes under physiological circumstances throughout time. Molecular docking studies cannot further understand this stability. Another purpose is to determine the status of the target protein, particularly whether folded or unfolded, by examining the RG graph generated throughout the simulation period. The lowest value shows the protein's folded condition, whereas the highest value reflects the protein's structural state when unfolded [34]. The analysis of RMSF was carried out with macro md_analyzeres, while the Molecular Mechanics Poisson-Boltzmann Surface Area (MMPBSA) used macro md_analyzebindenergy.

3. RESULTS AND DISCUSSION

Lipinski's Rules of Five and ADMET Studies

Lipinksi's Rule of Five determines and identifies a new drug candidate through permeability and absorption properties [27]. Furthermore, this screening step is performed to obtain the physical-chemical properties of the drug candidates. The rules are molecular mass ≤ 500 Da, hydrogen bond donor lesser than 5, hydrogen bond acceptor lesser than 10, and MlogP ≤5. The results of Lipinski's Rule of Five of bioactive compounds from *Moringa oleifera* are listed in **Table 1**.

The result of Lipinski's Rule of Five was violated by seven compounds from moringa leaves (*Moringa oliefera*), namely beta carotene, lupeol acetate, sitogluside, tocopherol, chlorogenic acid, beta-sitosterol, and myricetin (**Table 1**). Beta carotene and sitogluside have a molecular mass of more than 500 Da, which causes the distribution failure to the cell membrane when oral medication is administered. Vice versa, the adherence of the bioactive compounds to Lipinski's Rule of Five simplifies the distribution and penetrates the drug into the cell membranes. Meanwhile, MlogP relates to the hydrophobicity or lipophilicity of a drug candidate. The bioactive compound with a higher MlogP value tends to have hydrophobic properties. It leads to toxicity to the human body because the drug diffuses spreadly and is long retained in a lipid bilayer. Last, the violation of HBD lesser than ≤5 causes absorption difficulties of the drugs in the human body. Based on Lipinski's Rule of Five screening, all 18 bioactive compounds from *Moringa oliefera* unviolate the rules.

ADMET analysis aims to explore the pharmacokinetics and toxicity of drug candidates from moringa leaves that are orally consumed. Poor pharmacokinetics and toxicity are the primary sources of failure in drug development. In vitro research can be carried out more quickly, but the research results often need to match the in vivo results. In vivo research yields valuable results, but it is time-consuming and costly. Therefore, the in silico method is present to complement these data because it is fast and inexpensive [35]. This parameter predicts drug performance to reach the target in the human body (**Table 2**).

The drug absorption prediction was tested using %HIA and Caco-2 cells. The value of %HIA shows the ability of drug candidate absorption in the human intestine. Data in **Table 2** explained that most ADMET tests were in the 70-100 range, indicating they are well absorbed in the human body [23]. Moreover, Caco-2 cell modeling was conducted to predict the absorption ability of bioactive compounds through the oral route in vitro. The distribution property of drugs in the human body is seen from the Blood-Brain Barrier (BBB) and Plasma Protein Binding (PPB).

The PBB parameter is crucial in the drug design of anti-Alzheimer drugs because this test estimates the drug candidate's ability to relate to the central nervous system (CNS). A drug must reach the CNS and pass the BBB [8]. The function of BBB is to act as a barrier between systemic circulation and CNS, and the function of the barrier is to protect the brain [36]. In **Table 2**, in general, active compounds from moringa leaves show a BBB in the range of 2.0-0.1, and these values exhibit good absorption. Some compounds have BBB lesser than 0.1, which presents poor absorption [23]. Furthermore, PPB is described in percentage, whereas a value more significant than >90% indicates that the drug is bound chemically to blood plasma. PPB also gives information about efficacy and drug disposition.

Furthermore, the drug metabolism element involves the enzyme cytochrome P450 (CYP450), increasing drug solubility in the human body. The drugs consumed can act as substrates, inhibitors, and inducers. The CYP450 enzymes that play the most role in drug metabolism are CYP3A4 and CYP2D6 [37]. CYP3A4 is found primarily in the liver, kidney, lung, brain, endothelium, placenta, and lymphocytes, while CYP2D6 is found in the liver, brain, and heart [35]. Based on **Table 2**, it can be seen that most of the compounds originating from *Moringa oleifera* are predicted to be non-inhibitory against CYP2D6. In CYP3A4, most compounds from *Moringa oleifera* are inhibitors. **Table 2** describes toxicity predictions regarding two parameters: mutagens and carcinogens. The Ames test seeks to identify the bacteria in substances that induce DNA alterations [23]. Positive findings indicated that the substance may induce DNA mutation, and the compounds in **Table 2** all test positive for mutagens. Furthermore, most compounds showed negative results in mice, indicating they were non-carcinogenic. Slightly different from carcinogenic tests in rats, most of the compounds showed positive results [26].

Based on **Tables 1 and 2**, eighteen compounds should be calculated using molecular

docking calculations. All of these compounds do not break the Lipinski Rule of Five. This guideline is based on the similarities between medications taken orally to people. Compliance with Lipinski's rule is often linked to the drug's physicochemical qualities of water solubility and intestinal permeability. These two characteristics are significant in determining oral bioavailability. Lipinksi prediction is often used to reduce the occurrence of molecules with poor physicochemical qualities [25,38].

Table 1. Lipinski's Rule of Five of bioactive compound from moringa leaves (*Moringa oleifera)*

No	Compounds	Lipinski's Rule of Five					
		Molecular Mass 500 (DA)	MlogP 5	Hydrogen Bond Acceptor (HBA) 10	Hydrogen Bond Donor (HBD) 5	Violation of Lipinsksi	Druglike
1	Rivastigmine			Control			
2	1,3 Dibenzil Urea	279	-0.41	6	3	0	Unviolate
3	1,4 Naftokuinon	158	1.621	2	0	0	Unviolate
4	Beta Carotene	536	12.605	0	0	2	Violate
5	Caffeic Acid	180	1.195	4	3	0	Unviolate
6	Chlorogenic Acid	354	-0.645	9	6	1	Violate
7	Ellagic Acid	302	1.241	8	4	0	Unviolate
8	Gamma Amino Butyric	103	-0.190	3	3	0	Unviolate
9	Kaempferol	286	2.305	6	4	0	Unviolate
10	Lupeol Asetat	468	8.595	2	0	1	Violate
11	Niazimin	399	0.874	8	2	0	Unviolate
12	Niazirin	279	-0.041	6	3	0	Unviolate
13	Pterygospermine	406	4.139	4	0	0	Unviolate
14	Quercetin	302	2.010	7	5	0	Unviolate
15	Sitogluside	576	5.849	6	4	2	Violate
16	Tocopherol	430	8.840	2	1	1	Violate
17	Beta Sitesterol	414	8.024	1	1	1	Violate
18	Vanilin	152	1.213	3	1	0	Unviolate
19	Glucocochlearin	375	-0.220	10	5	0	Unviolate
20	Myricetin	318	1.716	8	6	1	Violate
21	Genistein	270	2.415	5	5	0	Unviolate
22	Moringyne	312	-0,739	7	4	0	Unviolate
23	Rhamnetin	316	2.313	7	4	0	Unviolate
24	Apigenin	270	2.419	5	3	0	Unviolate
25	Daizein	254	2.713	4	2	0	Unviolate
26	Ferulic Acid	194	1.498	4	2	0	Unviolate

Table 2. ADMET test of bioactive compounds from moringa leaves (*Moringa oleifera*)

No.	Compounds	Adsorption			Distribution		Metabolisme, Excretion		Toxicity		
		%HIA	Caco-2 (nm sec^{-1})	MDCK	BBB	%PPB	CYP 3A4 Inhibition	CYP 2D6 Inhibition	Ames Test Mutagenicity	Mouse Carcinogenicity	Rat Carcinogenicity
1	Rivastigmine	97.95	55.51	0.87	0.08	79.83	Non	Inhibitor	Mutagen	Negative	Negative
2	1,3 Dibenzil Urea	92.80	21.31	41.99	2.95	99.73	Non	Inhibitor	Mutagen	Positive	Negative
3	1,4 Naftokuinon	99.52	20.90	60.05	1.78	68.54	Inhibitor	Non	Mutagen	Negative	Positive
4	Ascorbic Acid	33.15	2.48	0.88	0.11	5.30	Inhibitor	Non	Mutagen	Negative	Negative
5	Ellagic Acid	61.39	20.48	17.29	0.32	88.40	Inhibitor	Non	Mutagen	Negative	Positive
6	Gamma Amino Butyric	73.32	18.02	4.04	0.24	24.75	Inhibitor	Non	Mutagen	Positive	Negative
7	Kaempferol	79.43	9.57	79.43	0.28	89.60	Inhibitor	Non	Mutagen	Negative	Positive
8	Niazimin	73.16	19.71	2.25	0.02	56.23	Non	Non	Mutagen	Negative	Negative
9	Niazirin	75.22	0.84	37.24	0.03	48.12	Non	Non	Mutagen	Negative	Negative
10	Pterygospermine	97.82	5.4.49	0.08	0.05	94.06	Non	Inhibitor	Non-mutagen	Positive	Negative
11	Quercetin	63.48	3.41	13.35	0.17	93.23	Inhibitor	Non	Mutagen	Negative	Positive
12	Vanillin	93.05	19.59	122.18	0.56	63.14	Inhibitor	Non	Mutagen	Negative	Positive
13	Glucocochlearin	11.99	0.336	17.02	0.08	21.33	Inhibitor	Non	Mutagen	Negative	Positive
14	Genistein	88.12	5.74	39.43	0.17	89.73	Inhibitor	Non	Mutagen	Negative	Positive
15	Moringyne	62.99	13.59	62.99	0.10	46.04	Non	Non	Mutagen	Negative	Negative
16	Rhamnetin	66.11	16.11	21.92	0.05	87.98	Inhibitor	Non	Mutagen	Negative	Positive
17	Apigenin	87.31	10.52	44.30	0.59	100.0	Inhibitor	Non	Mutagen	Positive	Positive
18	Daizein	92.64	2.48	42.99	0.93	95.56	Inhibitor	Non	Mutagen	Negative	Positive
19	Ferulic Acid	90.60	21.11	228.55	0.75	50.41	Non	Non	Mutagen	Negative	Positive

Molecular Docking Calculation

Molecular docking calculation in this study was started using redocking step both rivastigmine-AChE receptor interaction. The reason for using rivastigmine as a control drug is that it is USA FDA-approved and has a smaller half-life than donepezil. Rivastigmine is a safe synthetic chemical that has been designed to improve medicinal efficacy. This molecule is a derivative of the fundamental structure of physostigmine [18] and is one of the world's three anti-Alzheimer medications [39,40]. Rivastigmine is a cholinergic or parasympathomimetic substance that inhibits both AChE and butylcholinesterase (BuChE)[41]. Donepezil is a native ligand of AChE in 4EY7. The binding energy of rivastigmine with the AChE receptor is -7.77 Kcal mol^{-1}, which is bound by conventional hydrogen bonds to the amino acid residues PHE295 and TYR124 (See Figure 2.B.). In addition, previous research data states that the active site of AChE is divided into three, namely Catalytic active gorge (GLU334, SER203, HIS447), Long narrow aromatic gorge (TRP86, TYR133, ILE451, GLU202, and GLY448), and Peripheral anionic site (TRP286, PHE295, TYR124, ASP74, and SER125) [42]. Based on the three active sites of AChE, it is known that PHE295 and TYR124 are included in the active site of the Peripheral anionic site. The three types of AChE receptor active sites can also be used as comparative data for the research results in this study. The RMSD value of redocking the rivastigmine-AChE receptor complex was obtained at 1.68 Å, indicating the method is well-validated (**Figure 1**) [43]. **Figure 1** shows a good comparison position for the ligand before and after redocking. **Figure 1** shows the carbonyl oxygen atom as the binding atom for the amino acid residue in the AChE receptor's active site. The carbonyl oxygen atoms of both ligands are close together, but the amine group is positioned opposite.

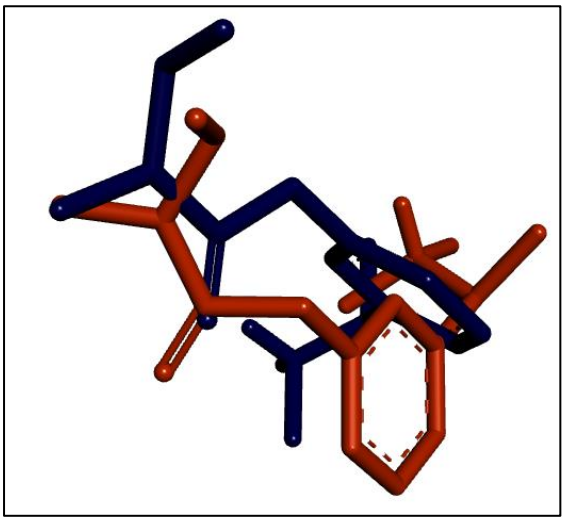

Figure 1. Comparison of rivastigmine in AChE (Dark blue before redocking and orange after redocking)

Table 3 contains 18 *Moringa oleifera* potential compounds selected from Lipinski's Rule of Five tests. The data proves that ten compounds have lower binding energies than the control ligand, namely 1,3 dibenzyl urea, ellagic acid, niazimin, niazirin, pterygospermine, glucocochlearin, rhamnetin, apigenin, and daizein. Information on inhibition constants (μM) can also provide significant information in studying ligand inhibitors against a disease. The lower predicted Ki value resulting from the calculation indicates that a small concentration is needed to inhibit a receptor[44].

Figure 2 explains in detail the interactions in the rivastigmine+AChE receptor complex. A three-dimensional visualization of the rivastigmine redocking against the AChE receptor is in **Figure 2A**. Inhibiting the AChE receptor involves creating a bond with the drug-candidate ligand in the receptor's active site. Conventional hydrogen bonds are the primary interactions that may enhance the binding energy generated [45]. Another secondary interaction is support, which enhances the intensity of the connection between the ligand and receptor at the active site [41]. The control ligand exhibits a conventional hydrogen bond with the amino acid residues TYR124 and PHE295 and linkage with five Van der Wals interactions against TYR337, VAL296, ASP74, GLY121, and SER125. Additionally, amino acid residues TYR341 and PHE338 stacked through π-π interactions. The π-sigma was noticed with TRP289, a carbon-hydrogen bond with ARG296, and PHE297 is π-acyl, respectively (**Figure 2B**). Conventional hydrogen bond is a primary interaction in molecular docking insight using Autodock Tools.

Figure 2C exhibits representative hydrogen bonds in the rivastigmine ligand area on the active site of the AChE receptor. The light purple area denotes a donor, while the green area is an acceptor. Amino acid residue PHE295 was linked to the carbonyl oxygen atom (2.17 Å), whereas TYR124 was to the amine rivastigmine group with a bond distance of 1.66 Å (**Figure 2.D**). The distance of PHE295 displayed a significant interaction with TYR124 to the active site of the AChE receptor. Therefore, drug candidates from *Moringa oleifera* were also calculated using a similar method for the AChE receptor to obtain crucial information (**Table 3**). **Table 3** shows that pterygospermine has the lowest binding energy as a potential anti-Alzeimer drug among all the compounds.

The potential drug pterygospermine has the lowest binding energy among the 18 compounds in **Table 5**. Based on molecular docking calculations, Pterygospermine has potential as a drug for an anti-Alzheimer alternative. The interaction of the pterygospermine with the AChE receptor is presented in **Figure 3**. The pterygospermine ligand revealed

conventional hydrogen bond interactions at amino acid residues TYR133 and GLU202. The mode of interaction of pterygospermine was different from that of the control ligand. However, both amino acid residues were included in the Long narrow aromatic gorge active site of the AChE receptor. Apart from that, ILE451, GLY120, GLY121, ASP74, GLY126, SER125, VAL194, PHE295, PHE297, TYR124, GLY448, and TRP286 exhibited Van der Wals interactions. The linkage π-π stacked was found between TYR341 and TRP86 to pterygospermine. While HIS447, TYR337, and PHE338 were linked to the active site of the ACHhE receptor as carbon-hydrogen bond interactions. In general, the bond distance of amino acid residues in the pterygospermine+AChE receptor complex is longer than the hydrogen bond distance in the rivastigmine+AChE receptor complex. In the pterygospermine-AChE receptor complex, the TYR133 was 2.53 Å to the active site. At the same time, GLU202 has a further distance from the active site in the AChE receptor (2.92 Å).

Table 3. Molecular docking calculations of bioactive compounds from Moringa leaves against AChE receptors

No.	Compounds	ID PubChem	Binding Energy (kcal mol^{-1})	Ki constant (μM)	Conventional hydrogen bond
1	Rivastugmine	77991	-7.77	1.83	PHE295, TYR124
2	1,3 Dibenzil Urea	72889	-8.04	1.29	ASP74
3	1,4 Naftokuinon	8530	-6.31	23.88	PHE338
4	Caffeic Acid	689043	-4.83	287.87	SER203
5	Ellagic Acid	5281855	-7.84	1.82	GLU202, SER203, ASN87, ASP74
6	Gamma Amino Butyric	119	-3.4	1.62	GLY122, SER203, HIS447
7	Kaempferol	5280863	-7.62	1.63	HIS447, TYR341, TYR337, ASP74, TYR124
8	Niazimin	129556	-8.13	1.09	HIS447
9	Niazirin		-8.10	6.30	GLU202, HIS447, PHE 295
10	Pterygospermine	72201063	-10.28	0.22	TYR133, GLU202
11	Quercetin	5280343	-7.59	2.71	TRP86, GLN71, HIS 447
12	Vaniline		-5.38	113.91	
13	Glucocochlearin	5281135	-9.18	185.10	GLU202, SER203, GLY120, GLY121, ALA203, GLY122, HIS447, SER125
14	Genistein	5280961	-8.54	545.94	TYR124, ARG296
15	Moringyne	131751186	-7.73		ASP74, THR83, TYR124
16	Rhamnetin	5281691	-8.9	1.17	ASP74, GLN71
17	Apigenin	5280443	-8.00	91.37	GLU202, GLY120, TYR72
18	Daizein	5391140	-8.47	613.46	GLY122, ARG296, SEER203
19	Ferulic Acid	445858	-5.22	150.29	SER203

Molecular Dynamics Simulation

Molecular dynamic simulation using YASARA Structure is a method to explore the ligand-protein complex's interaction dynamic in physiological conditions of 310K and pH 7.4. The salinity of physiological salt was used at 0.9%. This condition is strong enough to maintain the viability of the two samples. The analysis of potential energy had been obtained after running macro md_analyze. The analysis results from three samples generally showed that an average potential energy significantly increased from 0 ns to 0.5 ns running time (**Figure 4**). This data showed that the energy initiation reached energy stability. The energy fluctuation had happened even though the energy reached a stable potential energy (equilibrium phase). Increased energy fluctuation refers to the bonding strength of molecules, while the relaxation of molecular bonds causes decreased energy.

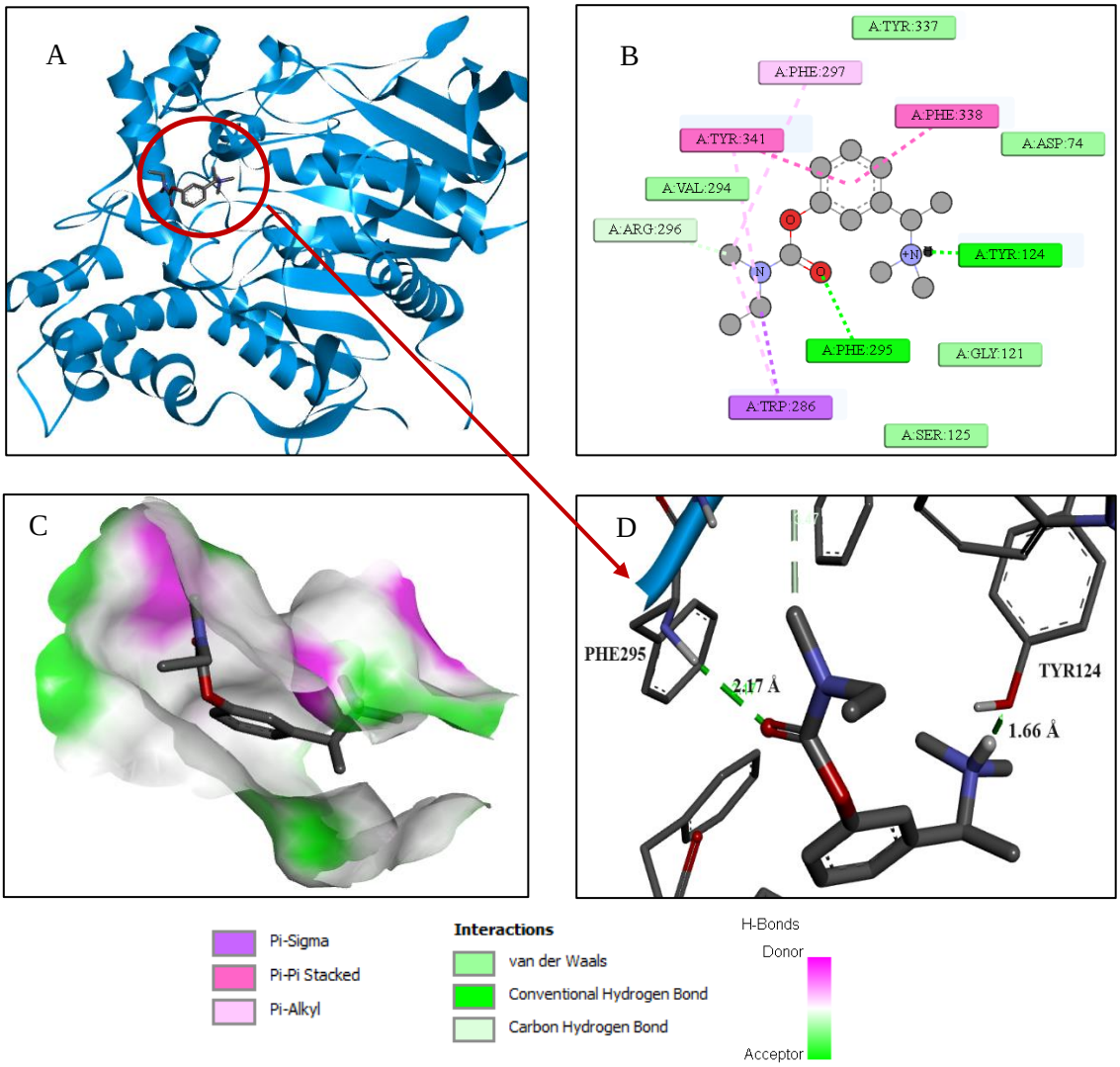

Figue 2. 3D visualization of the rivastigmine+AChE receptor complex (A), 2D visualization of the rivastigmine+AChE receptor complex (B), representative hydrogen bonds (C), and atomic interactions between rivastigmine and atoms of the AChE receptor amino acids (D). Apart from that, there is a legend that can explain the interactions that occur

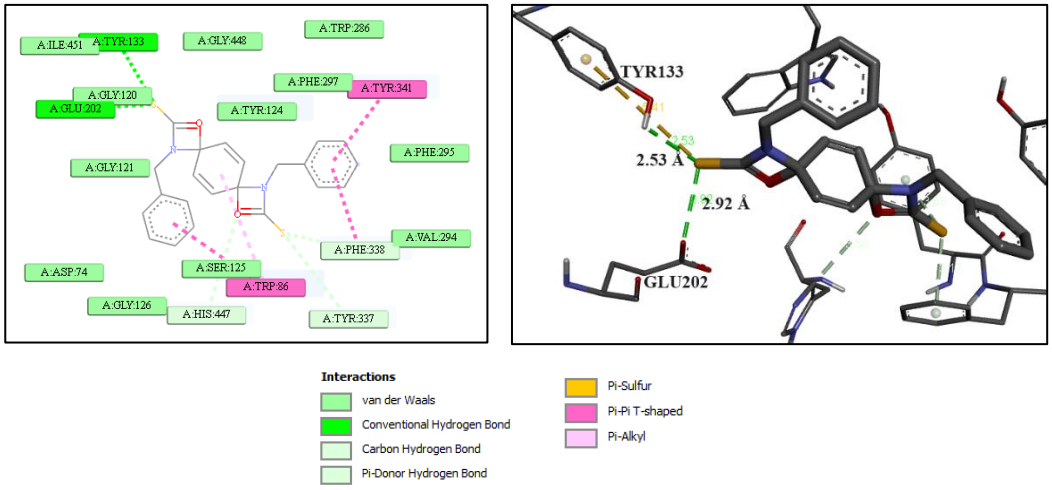

Figure 3. 2D visualization of the pterygospermine+AChE receptor complex (A) and the interaction of the pterygospermine ligand atoms with the amino acid residues of the AChE receptor (B)

Furthermore, MMPBSA analysis from rivastigmine showed that the energy average of the implicity solute during running 50 ns is 6.850 kJ mol^{-} and for pterygospermine is 37.377 kJ mol^{-1}, respectively (**Table 4**). In addition, higher binding energy also indicated a more compact interaction between ligand and protein, so pandamarilactonine F N-oxide was the most potential and expected ligand as an anti-Alzheimer agent [46–48]. The Molecular Mechanics Poisson-Boltzmann Surface Area (MMPBSA) energy was calculated based on the sum of the gas phase energy, solvation-free energy, and the contribution from the entropy configuration of the solute. The characteristic of the binding energy is closer to positive, the more stable and robust the binding energy in a complex [49]. The MMPBA calculation was performed based on the number of gas phase energy, free energy solvation, and configuration of solute entropy [49]. MMPBSA analysis is calculated using Eq. 1. Each average energy during 50 ns is shown in **Table 4**.

$$Bind\ Energy = EpotRecept + EsolvRecept + EpotLigand + EsolvLigand - EpotComplex - EsolvComplex\ [\ kJ\ mol^{-1}]$$

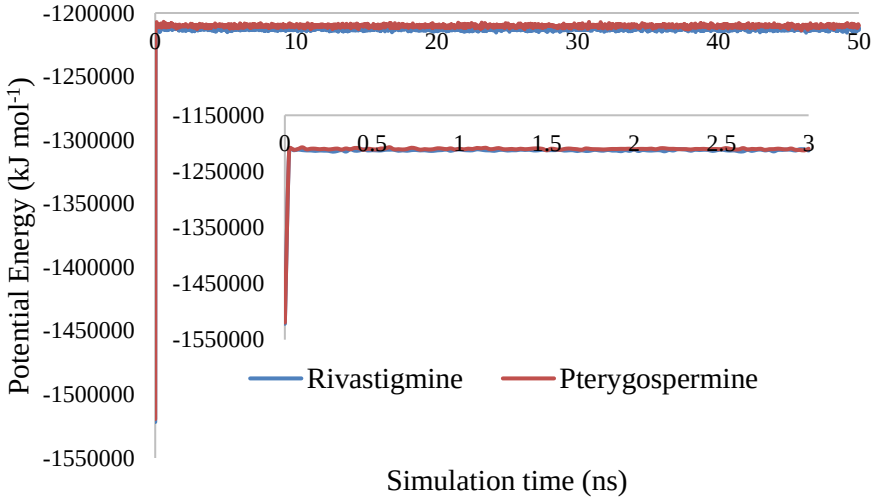

Figure 4. Potential energy of protein-ligand complex at 3 ns and 50 ns (blue line: rivastigmine and red line: pterygospermine)

Table 4. Components from MMPBSA equation

Energy	Rivastugmine Average	Pterygospermin Average
Epot Recept	-34265.211	-34255.981
Esolv Recept	-24426.497	-24565.717
Epot Ligand	32.802	-88.564
Esolv Ligand	-30.286	124.030
Epot Complex	-34265.220	-34255.983
Esolv Complex	-24430.822	-24567.627
Bind Energy [kJ mol^{-1}]	6.850	37.377

Total RMSD, RMSF, Ligand Configuration, and Radius of Gyration

Root Mean Square Deviation (RMSD) is an analysis score that provides conformation changes in macromolecules. This analysis also to predict the stability of ligand-protein combination in this study. Macromolecules act as receptors after an interaction with specific ligands. The RMSD analysis is obtained after running macro md_analyze. RMSD is also used as a deviation standard of conformation change. The value of RMSD is < 2Å generally applied to docking results [50]. RMSD data represents sample stability in simulation conditions where the conformation change is insignificant to dynamic stability. The meaning of dynamic stability is the absence of significant conformational changes, which is better known as the unfolding process. On the other hand, certain receptors resulting from the simulation have an RMSD of 3 Å, so this receptor system experiences significant conformation change from the native condition. **Figure 5A** shows the RMSD values for both stable samples with some fluctuations. Moreover, total RMSD of two samples revealed an average value of 2

Å, so the protein conformation in two samples was predicted not to change significantly.

The RMSD of the C-alpha protein for both samples was lower than the total RMSD value in **Figure 5B**. However, the Pterygospermine ligand showed an RMSD value that was not significantly different from that of rivastigmine as a positive control, indicating the potential nature of Pterygospermine as an AChE inhibitor. In addition to the RMSD of the entire molecule, the YASARA program can also be used to view the RMSD of the ligand configuration. The RMSD ligand analysis indicated that the ligand in the Rivastigmine complex is much more stable during the simulation time of 50 ns, with a range of 2-2.5 Å. Besides that, the pterygospermine ligand exhibited different dynamics than the rivastigmine ligand. At the initial simulation at 0-35 ns, the RMSD of the pterygospermine ligand was lower than the rivastigmine ligand. However, the system of the rivastigmine ligand experienced quite significant changes. This change was a significant conformational change, which induced the RMSD of the ligand to increase, ranging from 3-3.5 Å (**Figure 5C**). This condition can support the binding energy data, where pterygospermine has a more positive energy value than rivastigmine due to conformational changes in the pterygospermine ligand structure.

Radius of gyration (RG) analysis describes the equilibrium conformation of the entire simulation system. The RG value can also be explained as the radius of rotation of the dynamic movement of a protein-protein or protein-compound complex towards the solvent, so it is one way to predict the simulation of sample solubility in a solution or liquid solvent[34]. The lowest value indicates the folded condition of the protein, while the highest value indicates the conformational condition of the protein when it is unfolded [34]. The comparison results between the complexes show that the docking of the rivastigmine and pterygospermine ligands did not significantly change the RG pattern or that the protein was folded during the simulation time (**Figure 5D**).

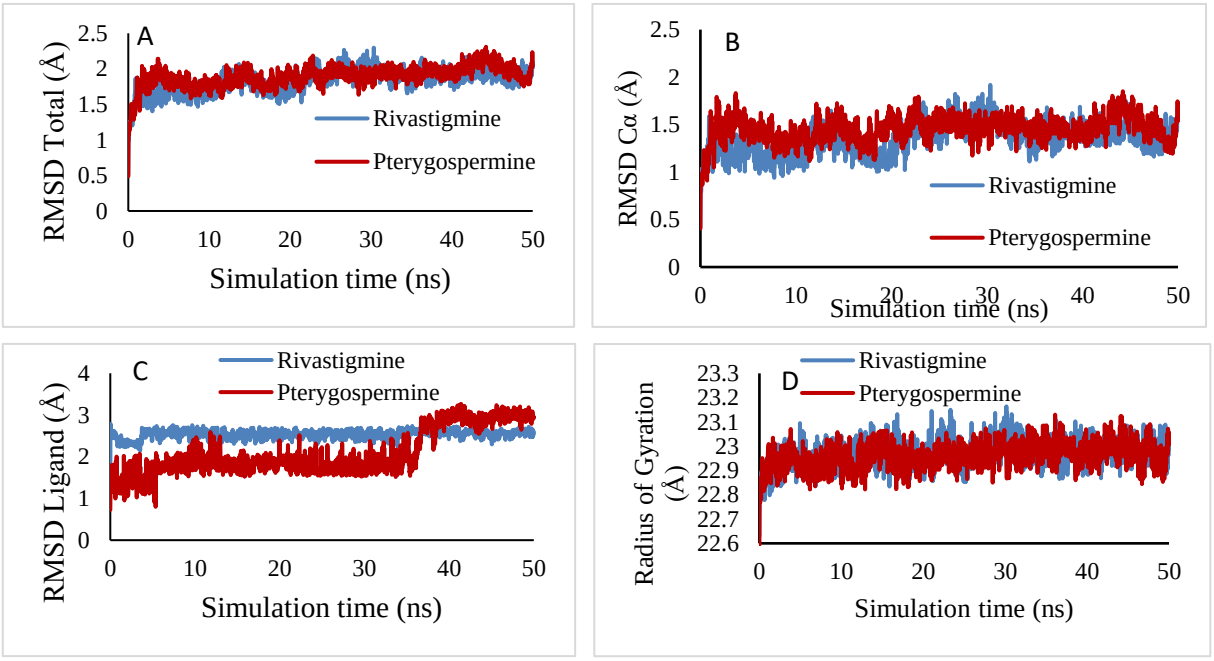

Figure 5. RMSD of rivastigmine and pterygospermine complexes to AChE (A), RMSD Cα of rivastugmine and pterygospermine complexes to AChE (B), RMSD of ligand configuration (C), dan Comparison of RG patterns between rivastigmine and pterygospermine complexes with AChE (D)

RMSF analysis of amino acid residue

Root Mean Square Fluctuation (RMSF) provides more detailed information on conformational changes because it is related to fluctuations at the level of amino acid and nucleotide residues of the ligand. RMSF data smaller than 3Å indicated favorable stability of ligand interactions with the enzyme, while high RMSF values induced deviations in the RMSD [46]. The RMSF results of the amino acid residues of the AChE protein structure in the rivastigmine and pterygospermine complexes show an average value of around 2 Å. In **Figure 6**, it can be seen that several amino acid residues have RMSF values that exceed 3 Å, so it is predicted that bond relaxation occurred in the target protein conformation, especially several residues with RMSF values above 4 Å. In general, amino acid residues have an RMSF smaller than 3 Å, while the RMSF of amino acid residues exceeding 3 Å represents a small amount. These amino acid residues

are GLU4, SER541, and ALA542. This information on amino acid residue was taken from analyses.

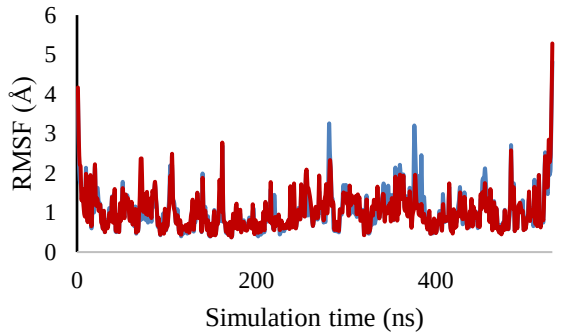

Figure 6. RMSF amino acid residues of AChE protein structure

4. CONCLUSIONS

Study of bioactive compounds from *Moringa oleifera* to AChE have been successfully investigated using ADMET properties, molecular docking, and molecular dynamics. The results of the screening stage obtained eighteen bioactive compounds for molecular docking calculations. Pterygospermine produces the lowest binding energy with hydrogen bond interactions at amino acid residues TYR133 and GLU202 in the active AChE site. A comparison of pterygospermine+AChE and rivastigmine+AChE complexes was simulated through molecular dynamics. The results of the comparison of the AChE complex with rivastigmine and pterygospermine show that the pterygospermine ligand has a stable interaction with AChE like the positive control (rivastigmine) against AChE based on RMSD and RMSF data. The Radius of Gyration analysis results do not show that the adding ligands can cause an unfolded effect on the protein. Based on the data, rivastigmine's binding energy is better than pterygospermine's because of the change in the conformation of the pterygospermine ligand during the simulation time. Although this study's findings clearly show of the interaction between ligand and receptor in AChE receptor inhibition, further in vitro and in vivo research is required to gain new insights into anti-Alzheimer's drug discovery.

ACKNOWLEDGMENTS

The author thanks Hafiz Aji Aziz for valuable discussions

REFERENCES

1. Karran E, De Strooper B. The Amyloid Hypothesis in Alzheimer Disease: New Insights from New Therapeutics. *Nat Rev Drug Discov*. 2022;21(4):306-318. doi:10.1038/s41573-022-00391-w
2. Pitchai A, Rajaretinam RK, Mani R, Nagarajan N. Molecular Interaction of Human Acetylcholinesterase with Trans-Tephrostachin and Derivatives for Alzheimer's Disease. *Heliyon*. 2020;6(9):e04930. doi:10.1016/j.heliyon.2020.e04930
3. Lima E, Medeiros J. Marine Organisms as Alkaloid Biosynthesizers of Potential Anti-Alzheimer Agents. *Mar Drugs*. 2022;20(1):1-26. doi:10.3390/md20010075
4. Kuzu B, Tan M, Taslimi P, et al. Mono- or Di-Substituted Imidazole Derivatives for Inhibition of Aetylcholine and Butyrylcholine Esterases. *Bioorg Chem*. 2019;86(October 2018):187-196. doi:10.1016/j.bioorg.2019.01.044
5. Wang L, Moraleda I, Iriepa I, et al. 5-Methyl-: N -(8-(5,6,7,8-tetrahydroacridin-9-ylamino)octyl)-5 H -indolo[2,3- b] quinolin-11-amine: A Highly Potent Human Cholinesterase Inhibitor. *Medchemcomm*. 2017;8(6):1307-1317. doi:10.1039/c7md00143f
6. Malik YA, Awad TA, Abdalla M, et al. Chalcone Scaffolds Exhibiting Acetylcholinesterase Enzyme Inhibition: Mechanistic and Computational Investigations. *Molecules*. 2022;27(10):1-17. doi:10.3390/molecules27103181
7. Tallini LR, Manfredini G, Rodríguez-Escobar ML, et al. The Anti-Cholinesterase Potential of Fifteen Different Species of *Narcissus* L . (Amaryllidaceae) Collected in Spain. *Life*. 2024;14(536):1-15. doi.org/10.3390/life1404053
8. Farihi A, Bouhrim M, Chigr F, et al. Exploring Medicinal Herbs' Therapeutic Potential and Molecular Docking Analysis for Compounds as Potential Inhibitors of Human Acetylcholinesterase in Alzheimer's Disease Treatment. *Med*. 2023;59(10). doi:10.3390/medicina59101812
9. Ghimire S, Subedi L, Acharya N, et al. *Moringa oleifera:* A Tree of Life as a Promising Medicinal Plant for Neurodegenerative Diseases. *J Agric Food Chem*. 2021;69(48):14358-14371. doi:10.1021/acs.jafc.1c04581
10. Balkrishna A, Misra LN. Ayurvedic Plants in Brain Disorders: The Herbal Hope. *J Tradit Med Clin Naturop*. 2017;06(02):1-9. doi:10.4172/2573-4555.1000221
11. Djiogue S, Kammogne IY, Etet PS, et al. Neuroprotective Effects of the Aqueous Extract of Leaves of Moringa oleifera Neuroprotective Effects of the Aqueous Extract of Leaves of *Moringa oleifera* (*Moringaceae*) in Scopolamine-Treated Rats. 2022;(June). doi:10.35248/0974-8369.22.14.474

12 Magaji UF, Sacan O, Yanardag R. Antilipase, Antiacetylcholinesterase and Antioxidant Activities of *Moringa oleifera* Extracts. *Rom All rights Reserv Rom Biotechnol Lett*. 2022;27(1):3208-3214. doi:10.25083/rbl/27.1/3208-3214

13. Azlan UK, Annuar NAK, Mediani A, et al. An Insight Into The Neuroprotective and Anti-neuroinflammatory Effects and Mechanisms of *Moringa oleifera*. *Front Pharmacol*. 2023;13(January):1-18. doi:10.3389/fphar.2022.1035220
14. Kou X, Li B, Olayanju JB, et al. Nutraceutical or Pharmacological Potential of *Moringa oleifera* Lam. *Nutrients*. 2018;10(3). doi:10.3390/nu10030343
15. Amat-Ur-rasool H, Ahmed M, Hasnain S, et al. In Silico Design of Dual-Binding Site Anti-Cholinesterase Phytochemical Heterodimers as Treatment Options for Alzheimer's Disease. *Curr Issues Mol Biol*. 2022;44(1):152-175. doi:10.3390/cimb44010012
16. Rocchetti G, Pagnossa JP, Blasi F, et al. Phenolic Profiling and In Vitro Bioactivity of *Moringa oleifera* Leaves as Affected by Different Extraction Solvents. *Food Res Int*. 2020;127. doi:10.1016/j.foodres.2019.108712
17. Mahaman YAR, Huang F, Wu M, et al. *Moringa Oleifera* Alleviates Homocysteine-Induced Alzheimer's Disease-Like Pathology and Cognitive Impairments. *J Alzheimer's Dis*. 2018;63(3):1141-1159. doi:10.3233/JAD-180091
18. Ludwig L, Seifert R. The decline in the clinical relevance of pilocarpine and physostigmine monitored in pharmacology textbooks from 1878 to 2023 : nine take - home messages for future (pharmacology) textbook authors. *Naunyn Schmiedebergs Arch Pharmacol*. 2024;(0123456789):1-23. doi:10.1007/s00210-024-03558-x
19. Manogna C, Margesan T. In Silico and Pharmacokinetic Studies of Glucomoringin from *Moringa oleifera* Root for Alzheimer's Disease Like Pathology. 2024;(September 2021). doi:10.2144/fsoa-2023-0255
20. Idoga ES, Ambali SF, Ayo JO, et al. Assessment of Antioxidant and Neuroprotective Activities of Methanol Extract of *Moringa oleifera* Lam. leaves in Subchronic Chlorpyrifos-Intoxicated Rats. *Comp Clin Path*. 2018;27(4):917-925. doi:10.1007/s00580-018-2682-9
21. Zhou J, Yang WS, Suo DQ, et al. *Moringa oleifera* Seed Extract Alleviates Scopolamine-Induced Learning and Memory Impairment in Mice. *Front Pharmacol*. 2018;9(APR):1-11. doi:10.3389/fphar.2018.00389
22. Ajala A, Eltayb WA, Abatyough TM, et al. In-silico Screening and ADMET evaluation of Therapeutic MAO-B Inhibitors against Parkinson Disease. *Intell Pharm*. 2023;(November 2023). doi:10.1016/j.ipha.2023.12.008
23. Kiruthiga N, Alagumuthu M, Selvinthanuja C, et al. Molecular Modelling, Synthesis and Evaluation of Flavone and Flavanone Scaffolds as Anti-inflammatory Agents. *Antiinflamm Antiallergy Agents Med Chem*. 2020;20(1):20-38. doi:10.2174/1871523019666200102112017
24. Mirza FJ, Zahid S, Amber S, et al. Multitargeted Molecular Docking and Dynamic Simulation Studies of Bioactive Compounds from *Rosmarinus officinalis* against Alzheimer's Disease. *Molecules*. 2022;27(21):1-18. doi:10.3390/molecules27217241
25. Lipinski CA. Lead- and drug-like compounds: The Rule-Of-Five Revolution. *Drug Discov Today Technol*. 2004;1(4):337-341. doi:10.1016/j.ddtec.2004.11.007
26. Nainwal LM, Shaququzzaman M, Akhter M, et al. Synthesis, ADMET Prediction and Reverse Screening Study of 3,4,5-trimethoxy Phenyl Ring Pendant Sulfur-Containing Cyanopyrimidine Derivatives As Promising Apoptosis Inducing Anticancer Agents. *Bioorg Chem*. 2020;104:104282. doi:10.1016/j.bioorg.2020.104282
27. Lipinski CA, Lombardo F, Dominy BW, et al. Experimental and Computational Approaches to Estimate Solubility and Permeability in Drug Discovery and Development Settings. *Adv Drug Deliv Rev*. 2012;64(SUPPL.):4-17. doi:10.1016/j.addr.2012.09.019
28. Pettersen EF, Goddard TD, Huang CC, et al. UCSF Chimera - A visualization System for Exploratory Research and Analysis. *J Comput Chem*. 2004;25(13):1605-1612. doi:10.1002/jcc.20084
29. Moss DE. Improving anti-neurodegenerative benefits of acetylcholinesterase inhibitors in alzheimer's disease: Are irreversible inhibitors the future? *Int J Mol Sci*. 2020;21(10):1-18. doi:10.3390/ijms21103438
30. Morris GM, Goodsell DS, Halliday RS, et al. Automated Docking using a Lamarckian Genetic Algorithm and An Empirical Binding Free Energy Function. *J Comput Chem*. 1998;19(14):1639-1662. doi:10.1002/(SICI)1096-987X(19981115)19:14<1639::AID-JCC10>3.0.CO;2-B

31. Gaarett M. Morris, Goodsell DS, Halliday RS, et al. AutoDock4 and AutoDock Tools4: Automated Docking with Selective Receptor Flexibility. *J Comput Chem*. 2012;32:174-182. doi:10.1002/jcc
32. Humble HL and MS. YASARA: A Tool to Obtain Structural Guidance in Biocatalytic Investigations. *Protein Eng*. 2017;1685:43-67.
33. Shakil S. Molecular Interaction of Inhibitors with Human Brain Butyrylcholinesterase. *EXCLI J*. 2021;20:1597-1607. doi:10.17179/excli2021-4418
34. Yamamoto E, Akimoto T, Mitsutake A, et al. Universal Relation between Instantaneous Diffusivity and Radius of Gyration of Proteins in Aqueous Solution. *Phys Rev Lett*. 2021;126(12):1-20. doi:10.1103/PhysRevLett.126.128101
35. Shin HK, Kang Y, No KT. 2016. *Predicting ADME Properties of Chemicals*. In Handbook of Computational Chemistry. Springer Science Business Media Dordrecht.
36. Daina A, Zoete V.A BOILED-Egg To Predict Gastrointestinal Absorption and Brain Penetration of Small Molecules. *ChemMedChem*. Published online 2016:1117-1121. doi:10.1002/cmdc.201600182
37. Zhai J, Man VH, Ji B, Cai L, Wang J. Comparison and summary of in silico prediction tools for CYP450-mediated drug metabolism. *Drug Discov Today*. 2023;28(10):103728. doi:10.1016/j.drudis.2023.103728
38. Mardianingrum R, Susilawati D, Ruswanto R. Computational Study of 1-(3-Nitrobenzoyloxymethyl)-5-Fluorouracil Derivatives as Colorectal Cancer Agents. *J Kim Val*. 2022;8(2):211-220. doi:10.15408/jkv.v8i2.25489
39. Allgaier M, Allgaier C. An update on Drug Treatment Options of Alzheimer's disease. *Frontiers Biosci*. 2014;19:1345-1354.
40. Rezaul Islam M, Akash S, Murshedul Islam M, et al. Alkaloids as drug leads in Alzheimer's treatment: Mechanistic and therapeutic insights. *Brain Res*. 2024;1834(February):148886. doi:10.1016/j.brainres.2024.148886
41. Jamal QMS, Khan MI, Alharbi AH, et al. Identification of Natural Compounds of the Apple as Inhibitors against Cholinesterase for the Treatment of Alzheimer's Disease: An In Silico Molecular Docking Simulation and ADMET Study. *Nutrients*. 2023;15(7). doi:10.3390/nu15071579
42. Peitzika SC, Pontiki E. A Review on Recent Approaches on Molecular Docking Studies of Novel Compounds Targeting Acetylcholinesterase in Alzheimer Disease. *Molecules*. 2023;28(3):1-28. doi:10.3390/molecules28031084
43. Huey R, Morris GM, Olson AJ, et al. A Semiempirical Free Energy Force Field with Charge-Based Desolvation. *J Comput Chem*. 2006;28(6):1145-1152.
44. Bouamrane S, Khaldan A, Alaqarbeh M, et al. Garlic as an effective antifungal inhibitor : A combination of reverse docking , molecular dynamics simulation , ADMET screening , DFT , and retrosynthesis studies. 2024;17(July 2023). https://doi.org/10.1016/j.arabjc.2024.105642
45. Maharani DA, Adelina R, Aini AQ, et al. Molecular Docking and Dynamic Simulation of *Erythrina fusca* Lour Chemical Compounds Targeting VEGFR-2 Receptor for Anti-Liver Cancer Activity. Published online 2024. doi:10.15408/jkv.v10i1.3
46. Irsal RAP, Gholam GM, Dwicesaria MA, et al. Computational Investigation of Y. *aloifolia* variegate as anti-Human Immunodeficiency Virus (HIV) Targeting HIV-1 Protease: A Multiscale In-Silico Exploration. *Pharmacol Res - Mod Chinese Med*. 2024;11(June):100451. doi:10.1016/j.prmcm.2024.100451
47. Mitra S, Dash R. Structural Dynamics and Quantum Mechanical Aspects of Shikonin Derivatives as CREBBP Bromodomain Inhibitors. *J Mol Graph Model*. 2018;83:42-52. doi:10.1016/j.jmgm.2018.04.014
48. Das B, Moumita S, Ghosh S, et al. Biosynthesis of Magnesium Oxide (MgO) Nanoflakes by using Leaf Extract of *Bauhinia purpurea* and Evaluation of Its Antibacterial Property Against *Staphylococcus aureus*. *Mater Sci Eng C*. 2018;91(May):436-444. doi:10.1016/j.msec.2018.05.059
49. Aldeghi M, Bodkin MJ, Knapp S, et al. Statistical Analysis on the Performance of Molecular Mechanics Poisson-Boltzmann Surface Area versus Absolute Binding Free Energy Calculations: Bromodomains as a Case Study. *J Chem Inf Model*. 2017;57(9):2203-2221. doi:10.1021/acs.jcim.7b00347
50. Trott A, Olson AJ. Software News and Updates Gabedit — A Graphical User Interface for Computational Chemistry Softwares. *J Comput Chem*. 2012;32:174-182. doi:10.1002/jc